Visual Quality Inspection and Fine Anomalies: Methods and Application

Simon-Frédéric Désage[1], Gilles Pitard[1], Maurice Pillet[1], Hugues Favrelière[1], Fabrice Frelin[1], Serge Samper[1,2], Gaëtan Le Goïc[1,3], Laurent Gwinner[4], and Pierre Jochum[4]

[1] SYMME, Laboratoire des Systèmes et Matériaux pour la Mécatronique, Université de Savoie, Annecy, France
{simon-frederic.desage,gilles.pitard,maurice.pillet, hugues.favreliere,fabrice.frelin,serge.samper, gaetan.legoic}@univ-savoie.fr
[2] LARMAUR ERL CNRS 6274, Laboratoire de Recherche en Mécanique Appliquée de l'Université de Rennes 1, Rennes, France
[3] LE2I, Laboratoire d'Electronique, Informatique et Image, UMR CNRS 6306, Auxerre, France
[4] CETEHOR, Département technique du comité Francéclat, Besançon, France
{l.gwinner,p.jochum}@cetehor.com

Abstract. This study develops a surface inspection methodology used to detect complex geometry products and metallic reflective surfaces imperfections. This work is based on combination of three complementary methods: an optical one (structured light information), an algorithmic one (data processing) and a statistical one (parameters processing). *A usual industrial application illustrates this processing.*

Keywords: Surface metrology, Quality Inspection, Computer Vision, Image Processing, Statistic.

1 Introduction

Even nowadays visual quality inspection is a problem. Inspected items have complex geometries, metallic reflective surfaces and high-added values. There have already been studies in industry to establish a methodology for quality inspection, particularly through the PhD works of Anne-Sophie Guerra [1], Nathalie Baudet [2] and Gaëtan Le Goïc [3]. These works helped to highlight the variability of human expert judgment (or controllers) during quality inspection processes [4]. The main objective is to eliminate over and under quality, by improving the controller's working conditions and thus, reduce costs for companies. Our method proposes to use an objective vision system calibrated with Human-based criteria. An example of fine defect automatic detection is presented. The choice of best processing parameters is optimized by design of experiments.

S. Ratchev (Ed.): IPAS 2014, IFIP AICT 435, pp. 94–106, 2014.

2 Background

2.1 Industrial Problem

Following the Anne-Sophie Guerra PhD [1 - p. 85-86] and Nathalie Baudet [2 - p.73], a generalized methodology was established for surface inspection. It consists of three main phases:

1) **Exploration phase:** Anomaly (ies) observation and research - Extraction.
2) **Evaluation phase:** Determination of anomaly criticality.
3) **Decision phase:** Determination of product overall acceptability.

The implementation of this methodology allows visual quality control of products . Through quality inspection, companies want to tighten their evaluation criteria to improve the quality of their products. This is based on the hypothesis that a human control is the best detection system.

That's why, in many companies, quality inspection is still done visually by human operators. This is often justified by the high optical anisotropy of surface appearance of controlled products. This is due either to product complex geometry or its surface texturing that interacts irregularly with light, or a combination of both.

These operators define human visual perception (or sensitivity) like a visual acceptability threshold of product surface appearance. Industrial problem of quality inspection is particularly sensitive to human judgment variability. Indeed, human sensitivity is different for the same person over time and depending upon the mood. Moreover, people have their own sensitivity and experience, which is also a source of variations in human controls. To reduce this variability, we propose a vision system and data processing methods to assist human controller for a more objective detection. We recommend observing an object on a screen in order to have the same view (standard observation) and to agree on the defect importance (criticality).

2.2 Anomalies and Classification

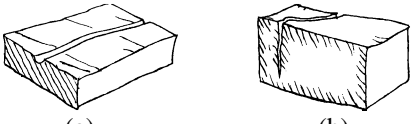

Fig. 1. (a) Example of stripe and (b) example of crack. [5]

We have established an easy classification of typical metal-surface products anomalies. Anomalies are defined as differences between studied cases and perfect model. A defect is an unacceptable anomaly. We distinguish two types of light behavior for surface anomalies. Indeed, metal products generally have two types of anomalies:

– The first type is **anomalies of bright appearance** relative to their immediate neighborhood. ***Stripes*** are a typical example (Figure 1a). These anomalies caused by design, manufacturing or even using.

– The second type is **anomalies of dark appearance** relative to their immediate neighborhood. ***Cracks*** are a typical example (Figure 1b). Unlike the first type, these anomalies are usually due to faulty manufacturing on small products. [6]

For both, we can see them when there is a high contrast. The difficulty for controllers is to find something that does not exist in a "normal" specimen. They must also be able to do so in such a configuration that replicates any potential orientation that would cause the defect to be unpleasant to the customer, and within a limited timeframe. Generally, either anomaly or its neighborhood blinds us, which is uncomfortable for our eyes.

2.3 Optics Data

Gaëtan le Goïc has applied the generalized methodology [3 - p.5-15] to metallic products. He proposes a visual inspection system (Figure 2), close to a photometric system, which allows a link with human perception [3 - p.126-131]. This system can provide all object views for a hemisphere of illumination, i.e. one view for one lighting incidence, while it is not certain that a human controller has control all of these configurations.

There is therefore an interest in optical systems that allow for an enhanced view of an object's appearance to improve his quality inspection. We made a distinction between vision systems that can observe three-dimensional objects and those that allow understanding object surface by shades of luminance. It is possible to have both in the same device.

For the first category, we can notice all systems as stereoscopy that using multiple shots and giving geometric shape. For the second category, the optical system is generally composed of a dome (hemispherical or almost a complete sphere) on which light sources are regularly distributed, and having a camera at the top of system. The interest of regular arrangement of light sources is to facilitate acquired data interpolation, and so as to understand object surface appearance.

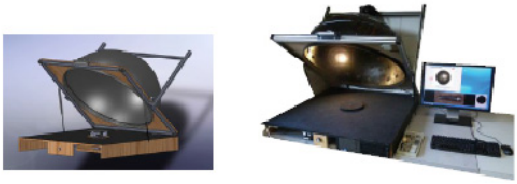

(a) (b)

Fig. 2. Surface Inspection Support Device, developed at the SYMME Laboratory. [3 –p.130]

The difficulty is to find a compromise between mathematical complexity and data volume, and to have reduced fitting function the closest. In other words, we want to keep photorealistic rendering and optimize memory volume. It should also take into account (spatial and electronic) device resolutions and its optical magnification.

In order to facilitate calculations, models have been used to approximate an interpolation function. We can cite two current types of interpolation:

– Polynomial interpolation (PTM) – [3] [7-9]

– Interpolation by spherical or hemispherical harmonics (SH or HSH) – [10-12]

All of these systems provide an object view in order to reach the first phase of quality inspection: the **"Exploration phase"**.

Moreover, we are working in collaboration with CETEHOR to deal with real cases of watch making with complex geometry, such as watch links. In order to facilitate a reduction in data volume, we used a system that incorporated interpolation. Many different object views can then be reduced to a subset configuration for anomaly detection. The quality criteria for watch links were agreed upon with an expert from CETEHOR.

3 Proposed Method: Structured Detection

3.1 The Image: Essential Data

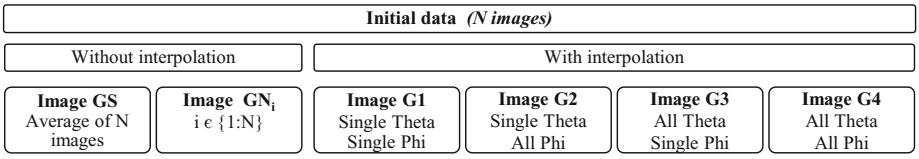

Fig. 3. Diagram of possible image data

We use several "classifications" of images:

- **GS**: That's the image of average rendering of acquired data.
- **GN$_i$**: That's one image from acquired data (number i ϵ {1:N}).
  Theta is azimuth and **Phi** is elevation of a hemisphere.
- **G1**: That's the object's rendering from a unique configuration of the three reference points (lighting - object - point of view), as a photo.
- **G2**: That's the object's rendering such as illuminated by a quarter of a vertical continuous circle of leds.
- **G3**: That's the object's rendering such as illuminated by a horizontal ring of leds.
- **G4**: That's the object's rendering such as illuminated by the whole hemisphere.

First, we need to extract or compose an image containing anomaly (ies). In the case of an "a priori" knowledge from product geometry, we can restrict research to a hemispherical space. There is already a system restricted to equivalent of two images G3 for flat objects (Figure 3) [13]. Any global specularity causing glare in the viewing system should be prohibited. In a first optimization, we can work with GS images and we can reduce the work area before filtering. We present a possible diagram (Figure 4) to define a relevant area and to obtain an image that we have labeled RS as reduced image. Its application is illustrated with the original image GS (Figure 5a), resulting image mask GM (Figure 5b) and reduced image RS (Figure 5c). For a complete analysis, the processing must be applied on each image G1.

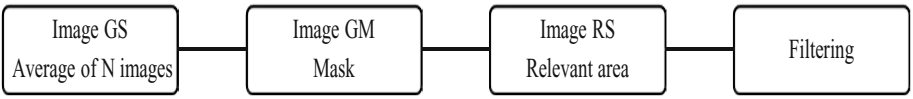

Fig. 4. Diagram of preprocessing before filtering

Fig. 5. Example of preprocessing before filtering

3.2 Detection Methods and Constraints

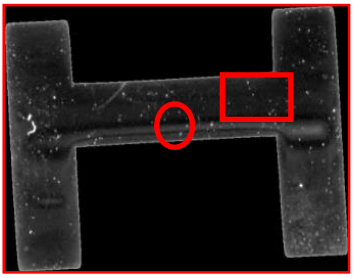

Fig. 6. Example of link of watch. Result of image RS combination and its mask. The viewing side is convex. Two remarkable things: a circle indicates dust and rectangle indicates a stripe. This stripe is evaluated by human controller as a "Strong mark".

Previous works have highlighted several techniques of image processing to detect fine anomalies. These are different combinations of filters such as the **"Top-hat"** [14] or the **"maximum opening"** [15-16], or the **"subtraction of maximum closure of opening by original image"** [17-18]. These methods are illustrated (Figure 7). These filters can easily and quickly become complicated. There are some states of the art for other detection methods such as road defects [6] or fabric defects [19]. For these reasons that is necessary to know characteristics of the object that are sought. These methods are derived from mathematical morphology to extract a local supremum (upper bound of local neighborhood) or a local infimum (lower bound of the local neighborhood). The local neighborhood is defined before processing by a structuring element.

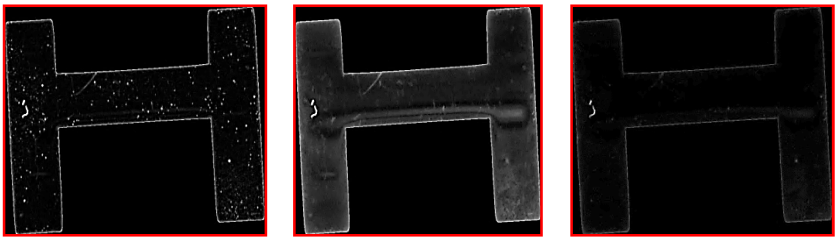

(a) (b) (c)

Fig. 7. Example of watch link. (a), (b) and (c) are filtering results of Figure 6. (a) by top-hat (b) by maximum opening and (c) by subtraction of maximum closure of opening by original image.

Structuring element is generally defined by its shape, its length, and, eventually, by direction. In our case, sought anomalies are called fine because they have a linear structure. The structuring element, consistent with these anomalies, will be linear. The mathematical operation then is to browse with the structuring element over the image represented by a matrix of received light data. The result of this is then a processed image. [20]

(a) (b) (c) (d)

Fig. 8. Example of structuring element. (a), (b) and (c) are line structuring elements with different orientation (0°, 10°, 45°). (d) is a disk structuring element.

First, a fine anomaly with linear structure has a dominant direction. Depending on the desired filter, the direction of the linear structuring element is either perpendicular or parallel to the anomaly direction. This implies that the direction choice of the linear structuring element is important relative to the anomaly direction. However, our optical system enables taking of pictures structured in relation to the object and the direction of the anomalies, which allows us to constrain the mathematical treatment dedicated to the anomalies detection.

3.3 Proposed Filtering

An anomaly is best revealed when illuminated from a direction perpendicular to its dominant direction. So, the processing can be limited to two directions, parallel and perpendicular to incident direction of light, depending on desired filtering. We can combine filtering operations to obtain information on anomalies as residual information of processing as shown (Figures 9-10). A “twisted” anomaly, consisting of multiple “dominant” directions, can be broken down into several sub-anomalies, and processed as the sum of partial directions.

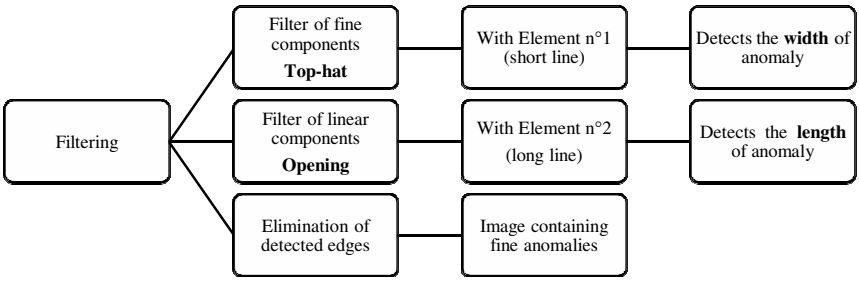

Fig. 9. Diagram of processing of filtering

Firstly, we apply a **Top-hat filter** with structuring element n°1 as a **low-pass filter** in the perpendicular direction to the dominant direction of anomalies. So, we keep elements with thin width in image. For images G1 or G2, we know the incident direction of light, so we can apply the filter in this direction because fine anomalies such as stripes are revealed for this incident direction of light. For images G3, G4 and GS, we must browse in different directions. Sometimes, it is interesting to process only for the four main directions as 0°, 45°, 90° and 135° ±180°.

Secondly, we apply **Opening filter** with structuring element n°2 as **high-pass filter** in parallel direction to the dominant direction of anomalies. So, we keep the elements with high height in the image. When we know incident direction of light, we can apply this filter in the perpendicular direction at the incident direction of light. The direction of this filter has 90° rotated from the Top-hat filter, as it has been hypothesized that fine anomalies have linear structure.

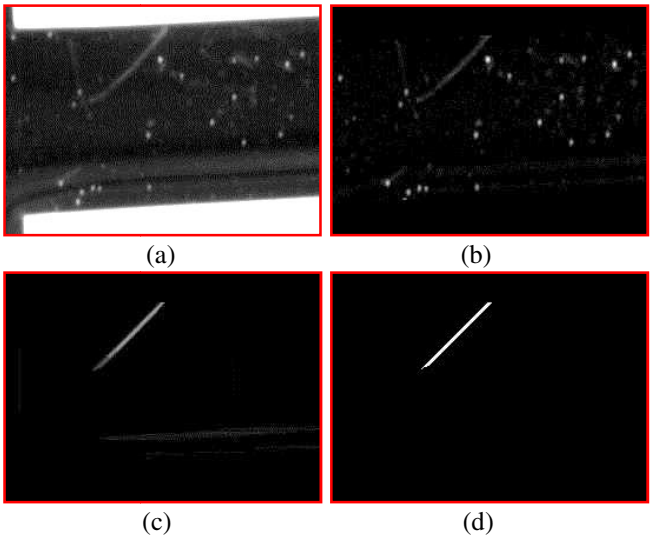

Fig. 10. Example of filtering with a region of interest of watch's link

We can also deduce the size scale for anomalies with a simple formula:

$$S = \left[\frac{FL}{WD} * \frac{SR}{SS} * CS \right] \quad (1)$$

Where S (pixels) is the structuring element size, WD (mm) is the working distance (camera-object distance), FL (mm) is the camera focal length, SS is the camera sensor size, SR (pixels) is the camera sensor resolution and CS (mm) is the crack appearance size. [19]

3.4 Optimization by Experimental Approach

Like the use of the design of experiments (DOE) method in the field of mechanics to optimize machining parameters [21], we want to use DOE to optimize the choice of the previous parameters, such as the characteristics of the element structuring. The objective is to obtain improved detection and thus facilitate evaluation of surface anomalies [22]. Indeed, this method is suitable when it comes to taking into account a large number of parameters and the relationship between them is not necessarily linear.

The capability to detect an anomaly depends of the structuring element parameters. These parameters are:

- The length of element 1 and element 2. The length of element 2 depends on length/width ratio of anomaly.
- The step of element's direction
- The mask of object

Factors		Levels				
		1	2	3	4	5
A	Mask	Without	Relevant area	Mask complete	Mask without edge (5 pixels)	Mask without edge (10 pixels)
B	Direction step	1°	3°	5°	15°	45°
C	Length of Element 1	5 pixels	10 pixels	15 pixels	20 pixels	25 pixels
D	Length of Element 2	2* Element 1	4*Element 1	6*Element 1	8*Element 1	10*Element 1

Fig. 11. Table settings

Using 5 levels per factor, the **full** factorial design is a 625 line table. We chose to make the fractional design L_{25} 5^6 with 25 trials. (Table 1, see Appendix)

The operation is to optimize two responses to find the best compromise. They are:

1. **The quality of detection**

The capability is a measure by comparison between the expert judgment on a

parts sample and the quality of the anomaly image. Note the ease of finding the anomaly identified by the expert in a scale from 0 to 10, (Figure 12a)

2. **The computation time**

Note the ease of process to identify anomaly in a scale of time (seconds) (Figure 12b)

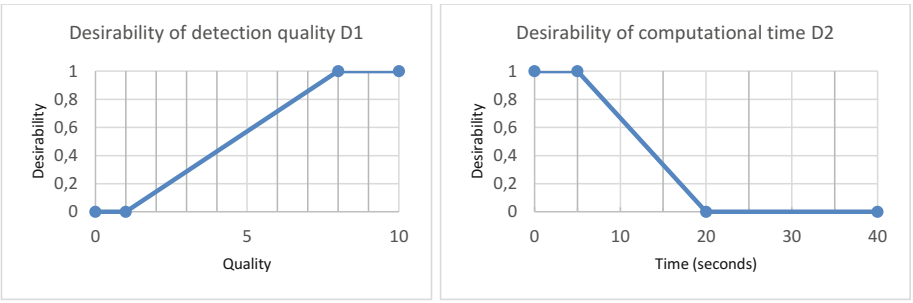

(a) (b)

Fig. 12. Desirability diagrams of detection, for quality and computational time

The overall desirability is calculated by the geometric mean of the two desirabilities:

$$OD = \sqrt[2]{D1.D2} \tag{2}$$

The overall desirability is as shown (Figure 15) and is the result of formula (2). The experiment is performed on five links with anomalies identified. The effects graph of quality response and time response are as shown (Figures 13-14). The local optima are surrounded by a red circle. For the parameter of the mask, it was obvious that the reduction of search area (of anomalies) would save computation time. However, the effects graph shows the reduction of the area may lead to wrong detection by generating false positives, such as edge detection.

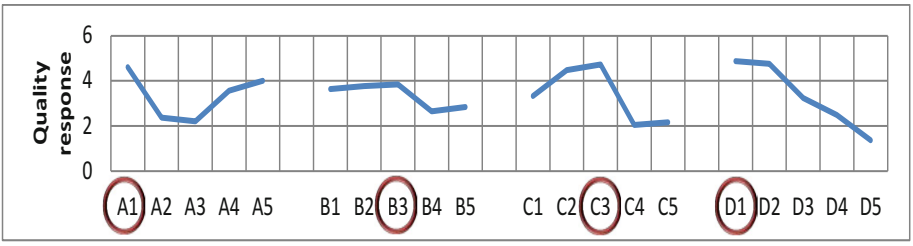

Fig. 13. Graph of the effects of quality response (average of 5 samples)

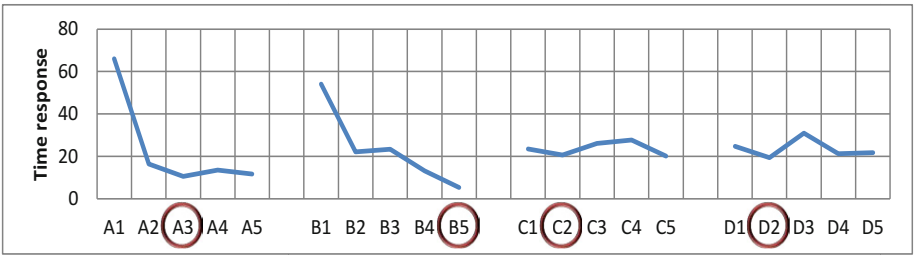

Fig. 14. Graph of the effects of time response (average of 5 samples)

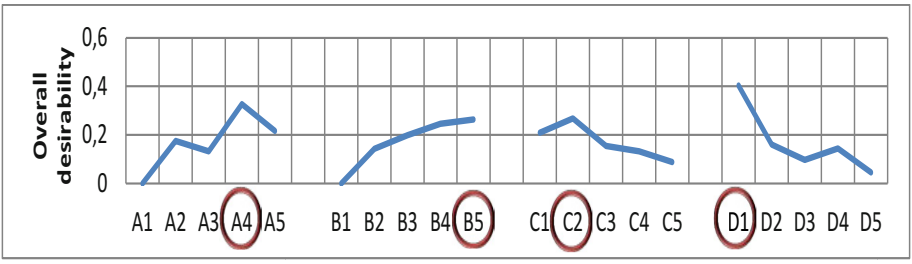

Fig. 15. Diagrams of overall desirability of detection (average of 5 samples)

The optimized parameters are **mask with trimmed edges 5 pixels**, a **step of 45 degrees**, a **length of 10 pixels for element 1** and a **width/length ratio of 2** to define length of element 2. These parameters are applied (Figure 16). The final image (Figure 16b) is used to assess the quality of the product based on the residual information it contains.

(a) (b)

Fig. 16. Example of optimized filtering, obtained in less than 4 seconds. (a) shows areas with visual impact on the links without edges and (b) is the result of threshold of these areas above half the maximum intensity.

With formula (1), we have an idea of appearance width of anomaly. The working distance (camera-object distance) is 440 mm, the camera focal length is 440 mm, the camera sensor size is 15.8 mm, the camera sensor resolution is 2136 pixels and the size of structuring element is between 10 and 15 pixels. So the appearance width is between 75 and 110 μm.

4 Conclusion

Following the methodology formalization of quality inspection, we are able to provide a theoretical meta-model and a physical system for visual exploration and detection of surface anomalies, including product reflective metal surface and those of complex geometry. The main objective is to reduce the overall variability of quality inspection of a product. In other words, we are able to determine the optimum optical system and data processing dedicated to controlling types of defects on one type of products. The main information of our publication is a combination of three methods (**optical - algorithmic - statistic**) to allow automatic detection of surface anomalies

The underlying information of our publication is that despite the advance of the effective methods, companies outside research still have little awareness. Here, we present an example of method that may be of interest in industrial production, but each method has been at least 5 years out of industry. The laboratory aims to transfer technological know-how, more or less mature, to improve industrial production. This means that research (academic) centres, technical centres, and companies must communicate with each other more.

Acknowledgments. We also wish to thank CETEHOR and companies have provided us the necessary samples to our research. We thank our partners in MESURA project as well as Arve Industries and Conseil General 74 to enable us to carry out this research by giving us resources.

References

1. Guerra, A.S.: Métrologie sensorielle dans le cadre du contrôle qualité visuel. Université de Savoie (2008), http://hal.archives-ouvertes.fr/tel-00362743/
2. Baudet, N.: Maitrise de la qualité visuelle des produits – Formalisation du processus d'expertise et proposition d'une approche robuste de contrôle visuel humain. Université de Grenoble (2012), http://tel.archives-ouvertes.fr/tel-00807304/
3. Le Goïc, G., Samper, S.: Système de détection d'anomalies d'aspect par la technique PTM (2011), http://hal.archives-ouvertes.fr/hal-00740313/
4. Baudet, N., Pillet, M., Maire, J.L.: Proposition d'une approche méthodologique pour réduire la variabilité dans le contrôle visuel à but esthétique. In: Proceeding of the International Conference on Surface Metrology, ICSM (2012), http://hal.univ-savoie.fr/hal-00740267/
5. ISO-8785 Geometrical Product Specification (GPS) – Surface Imperfection - Terms, definitions and parameters - International Organization for Standardization (1998)

6. Nguyen, T.S., et al.: Etude d'un algorithme de détection de défauts sur des images de chaussées. XXIIe colloque GRETSI (Signal and Image Processing). Dijon (2009), http://documents.irevues.inist.fr/handle/2042/29100
7. Dellepiane, M., et al.: High quality PTM acquisition: reflection transformation imaging for large objects. In: Proceedings of the 7th International Conference on Virtual Reality, Archeology and Intelligent Cultural Heritage (2006), http://dl.acm.org/citation.cfm?id=2384330
8. Duffy, S.: Polynomial texture mapping at roughting linn rock art site. In: Proceeding of the ISPRS Commission V Mid-Term Symposiumm'close range image measurement techniques (2010), http://www.isprs.org/proceedings/XXXVIII/part5/papers/159.pdf
9. Baril, J.: Modèles de representation multi-résolution pour le rendu photo-réaliste de matériaux complexes. Université Sciences et Technologies Bordeaux 1 (2010), http://hal.archives-ouvertes.fr/tel-00525125/
10. Palma, G.: Visual appareance: Reflectance transformation imaging, RTI (2013)
11. Tunwattanapong, B., et al.: Acquiring reflectance and shape from continuous spherical harmonic illumination. ACM Transactions on Graphics (TOG) 32(4) (2013)
12. Elhabian, S.Y., et al.: Towards efficient and compact phenomenological representation of arbitrary bidirectional surface reflectance. In: British Machine Vision Conference, Dundee (2011), http://mecca.louisville.edu/wwwcvip/research/publications/Pub_Pdf/2011/Shireen/Elhabian_BMVC2011.pdf
13. Zamuner, G.: Application of artificial vision to the quality inspection of surfaces of luxury products. Ecole Polytechnique Fédérale de Lausanne (2012)
14. Zheng, H., et al.: Automatic inspection of metallic surface defects using genetic algorithms. Journal of Materials Processing Technology (2002)
15. Morard, V.: Detection de structures fines par traitements d'images et apprentissage statistique: application au contrôle non destructif. Ecole nationale supérieur des Mines de Paris (2012), http://imanalyse.free.fr/publications/Morardi-2012-These.pdf
16. Morard, V., et al.: One-dimensional openings, granulometries and component trees in per pixel. IEEE Journal of Selected Topics in Signal Processing 6(7) (2012), doi:10.1109/JSTSP.2012.2201694
17. Jahanshahi, M.R., et al.: An innovative methodology for detection and quantification of cracks through incorporation of depth perception. Machine Vision and Application 24(2) (2011), doi:10.1007/s00138-011-0394-0
18. Jahanshahi, M.R., Masri, S.F.: A new methodology for non-contact accurate crack width measurement through photogrammetry for automated structural safety evaluation. Smart Materials and Structures 22(3) (2013), doi:10.1088/0964-1726
19. Ngan, H., et al.: Automated fabric defect detection – A review. Image and Vision Computing 29(7) (2011), doi:10.1016/j.imavis.2011.02.002
20. Serra, J.: Morphological filtering: An overview. Signal Processing 38(1) (1994), doi:10.1016/0165-1684(94)90052-3
21. Pillet, M.: Les plans d'expériences par la method Taguchi (2001), http://hal.archives-ouvertes.fr/hal-00470004/
22. Moon, H., Kim, J.: Intelligent crack detecting algorithm on the concrete crack image using neural network. In: Proceedings of the 28th ISARC (2011)

Appendix

Table 1. The fractional design $L_{25}\ 5^6$ with 25 trials

	N° Factor				Quality (0 - 10) Sample n°					Time (seconds) Sample n°				
Test n°	**A**	**B**	**C**	**D**	**1**	**2**	**3**	**4**	**5**	**1**	**2**	**3**	**4**	**5**
1	1	1	1	1	6	6	6	6	6	102,8	104	101	113	109
2	1	2	2	2	8	8	8	8	8	64,68	64	63	69,2	65,4
3	1	3	3	3	8	8	8	8	5	81,98	86	81	94,9	89
4	1	4	4	4	0	0	1	1	1	50,13	51	49	57,7	53,3
5	1	5	5	5	1	1	1	1	1	18,33	19	18	21,9	19,8
6	2	1	4	5	1	1	1	2	2	65,46	66	66	63,5	67,1
7	2	2	5	1	2	1	3	3	2	8,24	9	8,9	8,5	8,63
8	2	3	1	2	2	3	6	6	2	3,22	3,5	3,4	3,4	3,44
9	2	4	2	3	2	2	7	2	2	2,54	2,7	2,7	2,59	2,68
10	2	5	3	4	1	1	1	2	2	1,84	1,9	1,9	1,87	2
11	3	1	2	4	2	2	1	2	2	25,13	28	27	25,7	26,2
12	3	2	3	5	1	1	2	3	2	15,64	17	17	15,6	16,3
13	3	3	4	1	2	1	6	6	2	4,68	5	5	4,76	5,01
14	3	4	5	2	2	1	2	3	2	3,32	3,7	3,5	3,37	3,43
15	3	5	1	3	3	2	1	2	2	1,58	1,7	1,6	1,61	1,66
16	4	1	5	3	1	1	2	3	2	47	55	50	47,7	49,4
17	4	2	1	4	0	8	8	0	8	5,99	6,8	6,4	6,02	6,17
18	4	3	2	5	1	1	1	8	2	7,02	7,8	7,3	7,08	7,22
19	4	4	3	1	1	9	8	9	2	2,22	2,5	2,3	2,25	2,3
20	4	5	4	2	1	1	7	3	2	1,76	2	1,8	1,8	1,83
21	5	1	3	2	8	8	8	9	3	21,8	25	23	22,6	23,3
22	5	2	4	3	1	1	1	4	3	13,26	15	14	13,3	14,3
23	5	3	5	4	1	1	1	4	3	12,82	17	14	13,4	14,1
24	5	4	5	4	1	1	1	4	2	4,8	5,7	5,1	5,07	5,04
25	5	5	2	1	6	6	8	8	7	1,57	1,8	1,6	1,6	1,65